

# Spatial uniformity of responsivity for silicon, gallium nitride, germanium, and indium gallium arsenide photodiodes

*T. C. Larason and S. S. Bruce*

**Abstract.** For almost a decade, the National Institute of Standards and Technology (NIST) has supplied to its customers calibrated photodiode standards and special tests of photodetectors for absolute spectral responsivity from 200 nm to 1800 nm. During this time spatial responsivity measurements have been made on several dozen Hamamatsu silicon S1337-1010BQ photodiodes. We have found that the spatial responsivity changes with wavelength, sometimes significantly as the wavelength approaches the bandgap. The most significant changes appear to be caused by defects in the photodiode material and are not apparent over most of the wavelength region where the photodiode operates. The change in spatial uniformity with wavelength can significantly contribute to measurement uncertainties. These measurements have been repeated and the spatial responsivities have remained constant over several years. Measurements have also been made on other types of Si, GaN, Ge, and InGaAs photodiodes. The measurement equipment, method, and results are presented.

## 1. Introduction

The National Institute of Standards and Technology (NIST) provides responsivity measurements of photodetectors over the 200 nm to 1800 nm spectral range [1]. The responsivity measurement method requires that the detector be underfilled and have a spatially uniform responsivity over the beam area. Starting in 1989, the silicon photodiodes (Hamamatsu S1337-1010BQ) provided by the NIST were measured for spatial uniformity of responsivity at 500 nm. In the early 1990s, it was found that many silicon photodiodes have a significant change in the uniformity as a function of wavelength, particularly as the wavelength approached the bandgap (1100 nm). This caused larger than expected uncertainties since the reproducibility of the responsivity measurement depends in large part on realignment to the same area of the photodiode. Also, changes in responsivity with geometry may not be correctly accounted for by using the uniformity data only at 500 nm if there are significant changes at wavelengths near the bandgap.

Since 1993, several dozen Hamamatsu S1337-1010BQ photodiodes have been measured at 500 nm

and 1000 nm. Some diodes had significant spatial non-uniformity at 1000 nm that was not evident at 500 nm. A few of these diodes have been remeasured over several years and the spatial non-uniformities have remained constant. This paper presents spatial uniformity data obtained during the past several years for the Hamamatsu S1337-1010BQ photodiode, plus data for several other photodiodes: Hamamatsu S1227-1010BQ and S2281 Si photodiodes, UDT Sensors UV100 Si photodiodes, International Radiation Devices (IRD) UVG-100 Si photodiodes, EG&G Judson J16TE2-8A6-R05M-SC thermoelectrically cooled Ge photodiodes, Telcom Devices 35PD5M-TO InGaAs photodiodes, and one APA Optics GaN photodiode.

The purpose of this paper is to catalogue typical spatial uniformities of various photodiodes. Spatial uniformity of photodiode responsivity has been reported in several papers [2-7]. Two papers have suggested different methods to quantify the uniformity [8, 9]. Non-uniformity is due to inhomogeneity in the photodiode material – typically inhomogeneity in surface recombination centres at shorter wavelengths [10, 11] and bulk recombination centres at longer wavelengths [12]. The non-uniformity near the bandgap has also been related to the (non-)uniformity of the bonding material's reflectance [13]. Because the semiconductor is almost transparent near the bandgap, changes in spatial reflectivity of the bonding material affect the amount of light reflected and therefore the responsivity of the photodiode.

---

T. C. Larason and S. S. Bruce: National Institute of Standards and Technology, Optical Technology Division, 221/B208, Gaithersburg, MD 20899-0001, USA.  
telephone: (301) 975-2334; fax: (301) 869-5700  
e-mail: thomas.larason@nist.gov

## 2. Experimental procedure

The spatial uniformity was measured by the two monochromator-based systems used for the spectral responsivity measurement service provided by the NIST. The measurements at 400 nm and above were performed using the Visible to Near Infrared Spectral Comparator Facility (VIS/NIR SCF). Those measurements below 400 nm were performed using the Ultraviolet Spectral Comparator Facility (UV SCF). A 100 W quartz-halogen lamp was used as the source in the VIS/NIR SCF and an argon arc was used as the source in the UV SCF. Variations in the source intensity for both SCFs were corrected by using a flat quartz plate as a beam splitter and a monitor detector after the monochromators. A Hamamatsu S1337-1010BQ silicon photodiode was used as the monitor over the spectral range 400 nm to 1000 nm. An EG&G Judson J16TE2-8A6-R05M-SC germanium photodiode was used as the monitor for near-IR measurements with the Ge and InGaAs photodiodes. For measurements below 400 nm, a UDT Sensors UV100 silicon photodiode was used as the monitor.

The VIS/NIR SCF uses a prism-grating monochromator, a NIST-modified Cary-14, which employs a 30° fused-silica prism in series with a 600 line/mm echelette grating. The monochromator's spectral range is 186 nm to 2.65  $\mu\text{m}$ . The spectral range used in the detector characterization facility is 350 nm to 1800 nm. In the typical measurement configuration, the monochromator slits are set to 1.1 mm with a bandpass of 4 nm. A circular aperture of 1.1 mm diameter just after the exit slit determines the beam size. The exit beam is  $f/9$ . The optical beam at the detectors is formed by a system of mirrors that image the exit aperture of the monochromator with 1:1 magnification. The monochromator has a stray light rejection of  $10^{-8}$ . Over 99% of the beam flux lies within an area of 1.6 mm diameter around the optical axis.

The UV SCF uses a Spex 1680, 0.25 m, double-grating monochromator. The spectral range of the monochromator is 180 nm to 1000 nm. The spectral range used in the detector characterization facility is 200 nm to 500 nm. In the typical measurement configuration, the entrance and exit slits are circular 1.5 mm diameter apertures with a bandpass of 4 nm. The exit beam is  $f/5$ . The optical beam at the detectors is formed by a system of mirrors that image the exit aperture of the monochromator with 1:1 magnification. Over 99% of the beam flux lies within an oval shape on the detectors of 2.5 mm by 2.0 mm around the optical axis.

Each SCF uses a pair of orthogonal linear-positioning stages to translate the detectors. The travel range of the VIS/NIR SCF horizontal stage is 400 mm with a resolution of 0.1  $\mu\text{m}$  and an accuracy of 0.2  $\mu\text{m}$  per 100 mm. The VIS/NIR SCF vertical stage and the UV SCF stages have a travel range of 50 mm with

a resolution of 0.1  $\mu\text{m}$  and an accuracy of 0.25  $\mu\text{m}$  per 25 mm. Each detector is mounted to allow its position to be adjusted along the optical axis. A gimbal mount allows the rotation and tilt of each detector to be adjusted for perpendicular alignment to the optical axis.

The spatial uniformity measurement procedures were the same for both the UV SCF and the VIS/NIR SCF. The detectors were aligned perpendicular to the optical axis using the He-Ne beam, positioned at the focal plane and aligned to the centre of the photodiode. A typical measurement consists of setting the monochromator to the desired wavelength and, for a 1  $\text{cm}^2$  test detector, scanning a 12 mm  $\times$  12 mm area in 0.5 mm steps. The test detectors were operated unbiased (the photovoltaic or short-circuit mode) and the signal was measured with a calibrated transimpedance amplifier and digital voltmeter (DVM). The amplifier gain for the test detector is typically  $10^6$ . The ratio of the test to monitor detector signals was stored on a computer for subsequent analysis. The spatial shape of the optical beam was assumed to be constant during the measurement.

The scans are always in the same horizontal direction; and the vertical direction is reversed in a "raster" scan, starting in the upper-left corner moving to the lower-right corner of the photodiode. Scanning horizontally in only one direction puts the stage drive against the same side of the drive screw. For the vertical scan, gravity keeps the stage always against the same side of the screw. This reduces hysteresis in the movement of the stages. The scan is large enough for the beam to move completely off the active area.

The ratios of the test to monitor detector signals are normalized to the mean of the centre ratios. The reported responsivity spatial uniformity surface is constructed from these normalized ratios. The relative measurement uncertainty [14] is the average standard deviation of the mean of the measurements in the centre of the active area of the detector. The combined standard uncertainty is the quadratic sum of the relative measurement uncertainty and the one-day DVM uncertainty specification. The relative standard measurement uncertainty ranged from  $10^{-5}$  to  $10^{-4}$ .

## 3. Results

The spatial uniformity of approximately one hundred Hamamatsu S1337-1010BQ 1  $\text{cm}^2$  photodiodes have been measured since 1989. Figure 1 shows a comparison of a Hamamatsu S1337-1010BQ spatial uniformity at two different wavelengths. The spatial uniformity measured in 1997 at 500 nm and 1000 nm is shown in Figures 1a and 1b, respectively. The spatial uniformity was also measured at 500 nm and 1000 nm in 1993. Changes in the uniformities are not noticeable on the scale of Figure 1. The two sets of measurements had an average difference at 500 nm of  $10^{-5}$  with a standard deviation of  $3.3 \times 10^{-4}$ . The average difference at

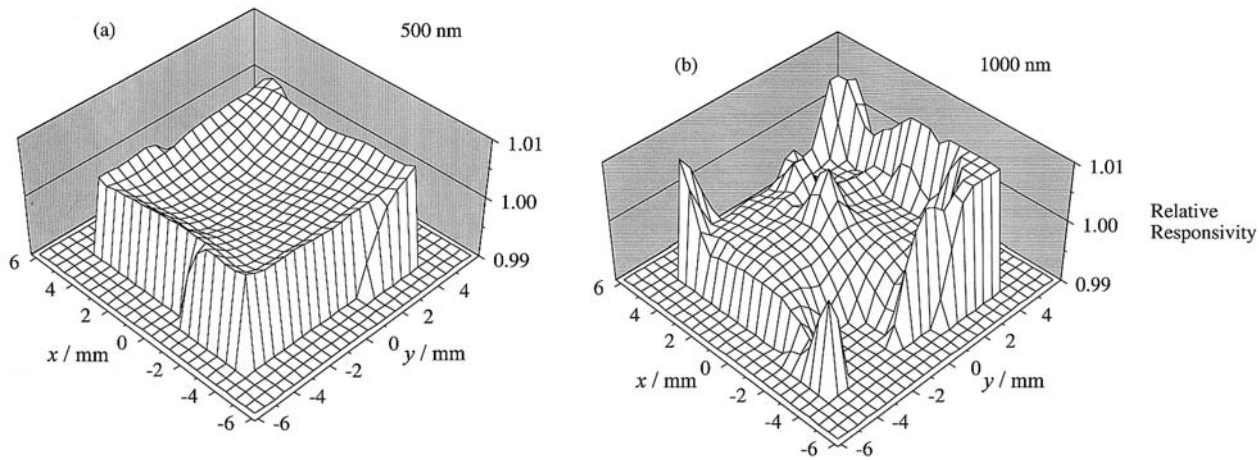


**Figure 1.** Comparison of Hamamatsu S1337-1010BQ #1 spatial uniformity with wavelength. Spatial uniformity measured at (a) 500 nm and (b) 1000 nm in 1997.

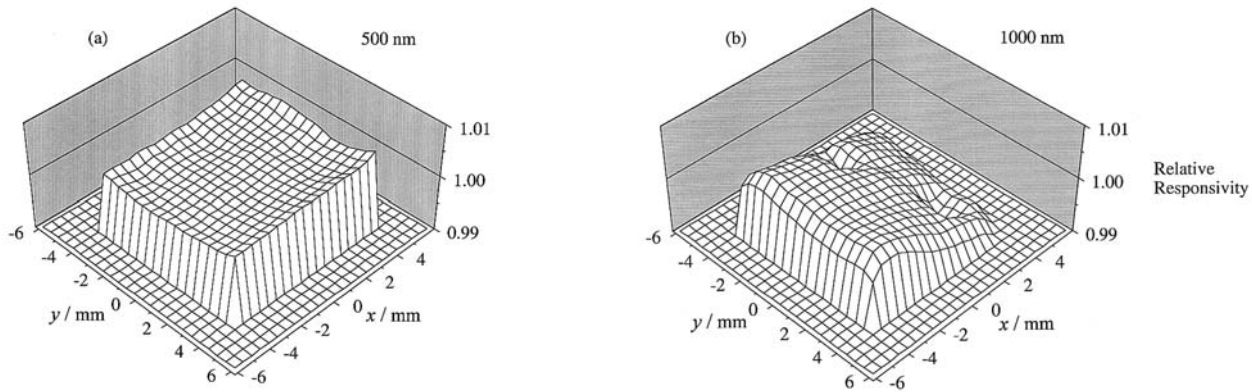


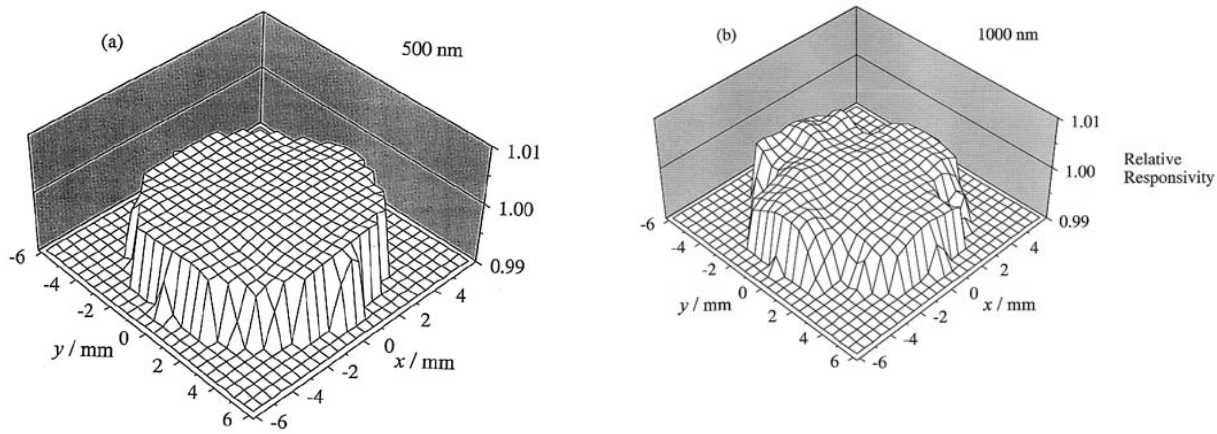
**Figure 2.** Comparison of Hamamatsu S1337-1010BQ #2 spatial uniformity at (a) 500 nm and (b) 1000 nm. This illustrates the typical uniformity for S1337-1010BQ photodiodes used as transfer standards.

1000 nm was  $6 \times 10^{-4}$  with a standard deviation of  $2.5 \times 10^{-3}$ . The changes seen are believed to result from errors when repeating positionings of the photodiode. The uniformity was concluded to be stable.

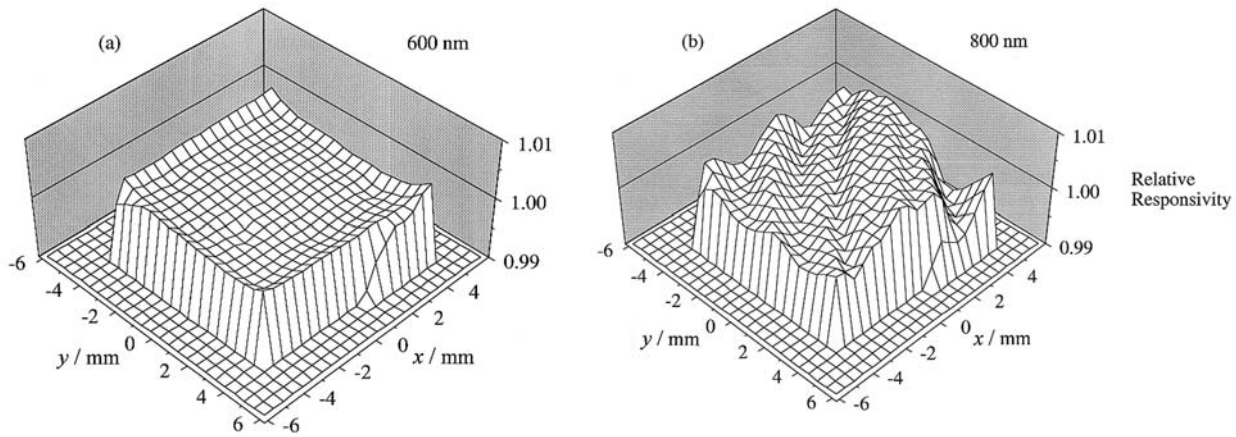
Figure 2 is a second example of the Hamamatsu S1337-1010BQ spatial uniformity at (a) 500 nm and (b) 1000 nm. The central portion of each diode at 500 nm is reasonably uniform, but Figure 1 reveals large non-uniformities at 1000 nm. Similar non-uniformities in other Hamamatsu S1337-1010BQ photodiodes of the order of 1% to 2% have been observed. Figure 2b shows a typical uniformity at 1000 nm. Approximately twenty-five Hamamatsu S2281 1 cm<sup>2</sup> photodiodes have been measured since 1995. Figures 3a and 3b show the spatial uniformities of a Hamamatsu S2281 photodiode at 500 nm and 1000 nm, respectively. This photodiode has a spectral responsivity almost identical to the S1337 series. The major difference is that the active area of the S2281 is round and it is supplied by the manufacturer in an integral BNC package.

Figure 4 is an example of the Hamamatsu S1227-1010BQ 1 cm<sup>2</sup> silicon photodiode spatial uniformity at (a) 600 nm and (b) 800 nm showing the typical uniformity measured. Non-uniformities of the order of 1% to 2% have also been observed at 800 nm for the Hamamatsu S1227-1010BQ. Approximately twenty Hamamatsu S1227-1010BQs have been measured since 1993. Figure 5 shows the spatial uniformity of the UDT Sensors UV100 1 cm<sup>2</sup> silicon photodiode that the NIST uses for the 200 nm to 450 nm spectral region. Figure 5a is the spatial uniformity measured at 250 nm and Figure 5b is measured at 350 nm. Approximately sixty UV100 photodiodes have been measured since 1990.

Approximately ten EG&G Judson Ge photodiodes have been measured since 1994. These detectors all had windows with a 20' wedge angle mounted 2° out of parallel with the photodiode and were measured at -30°C. The spatial uniformity at 1000 nm and 1600 nm for a typical EG&G Judson J16TE2-8A6-R05M-SC



**Figure 3.** Comparison of Hamamatsu S2281 #1 spatial uniformity at (a) 500 nm and (b) 1000 nm. This illustrates the typical uniformity for S2281 photodiodes used as transfer standards.



**Figure 4.** Comparison of Hamamatsu S1227-1010BQ #1 spatial uniformity at (a) 600 nm and (b) 800 nm. This uniformity was typical of most S1227-1010BQ photodiodes measured.

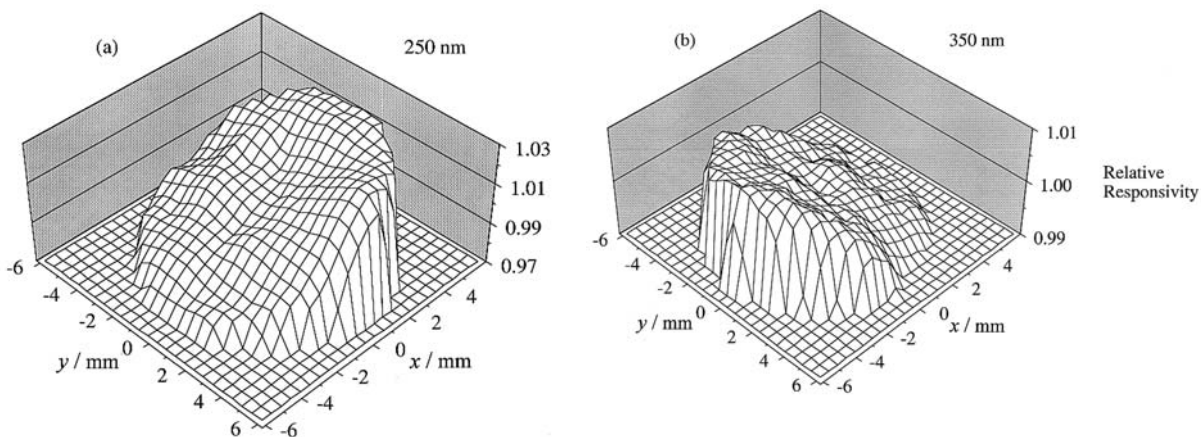


**Figure 5.** Comparison of UDT Sensors UV100 #1 spatial uniformity at (a) 250 nm and (b) 350 nm. This illustrates the typical uniformity for UV100 photodiodes used as transfer standards. Note the vertical scale change for (b).

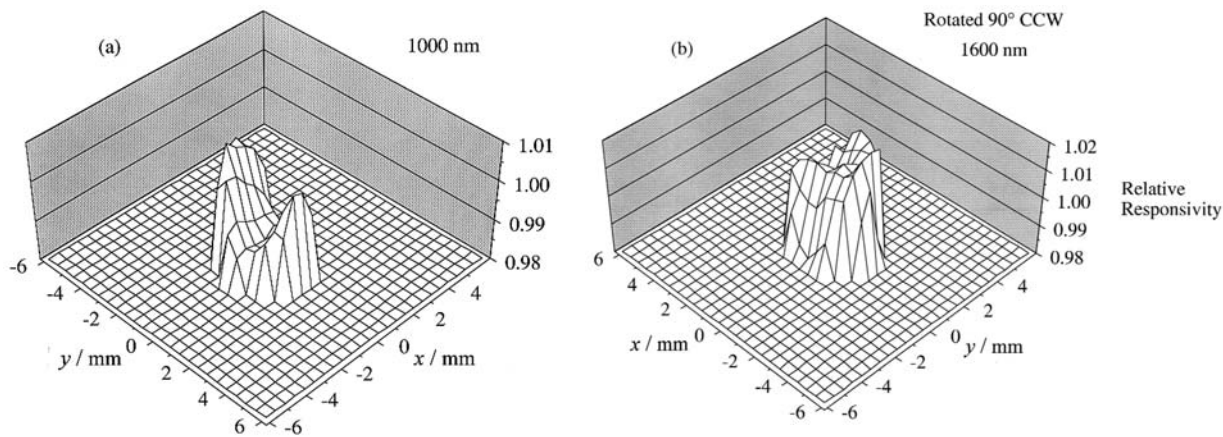


**Figure 6.** Comparison of EG&G Judson J16TE2-8A6-R05M-SC TE cooled Ge #1 spatial uniformity at (a) 1000 nm and (b) 1600 nm. Note that (b) is rotated 90° counter-clockwise and the vertical scale has changed.

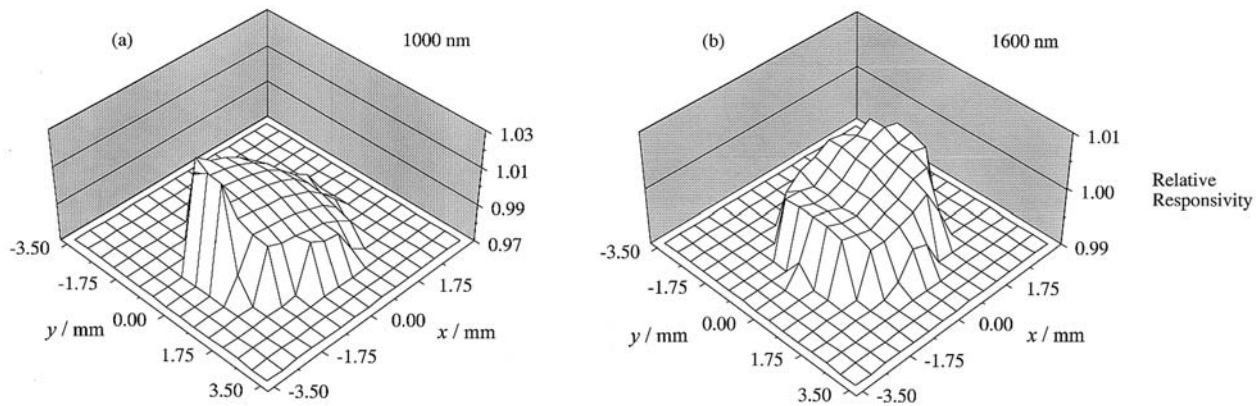


**Figure 7.** Comparison of Telcom Devices 35PD5M-TO InGaAs #1 spatial uniformity at (a) 1000 nm and (b) 1600 nm. Note the vertical scale change for (b). This uniformity was typical of the four 35PD5M-TO photodiodes measured.

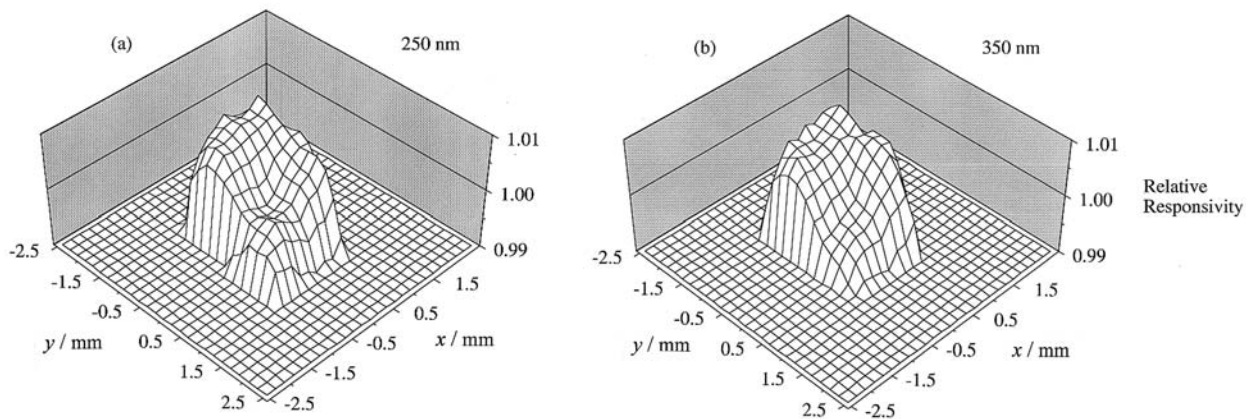


**Figure 8.** Comparison of APA Optics GaN #1 spatial uniformity at (a) 250 nm and (b) 350 nm.

thermoelectrically cooled 20 mm<sup>2</sup> Ge photodiode is shown in Figures 6a and 6b, respectively. Figure 6b is rotated 90° counter-clockwise for clearer presentation of the sloping uniformity. Figure 6 depicts the typical

uniformity measured. Figures 7a and 7b show a Telcom Devices 35PD5M-TO 20 mm<sup>2</sup> InGaAs photodiode at 1000 nm and 1600 nm, respectively. Figure 7 is typical of the four photodiodes of this type measured in 1997.

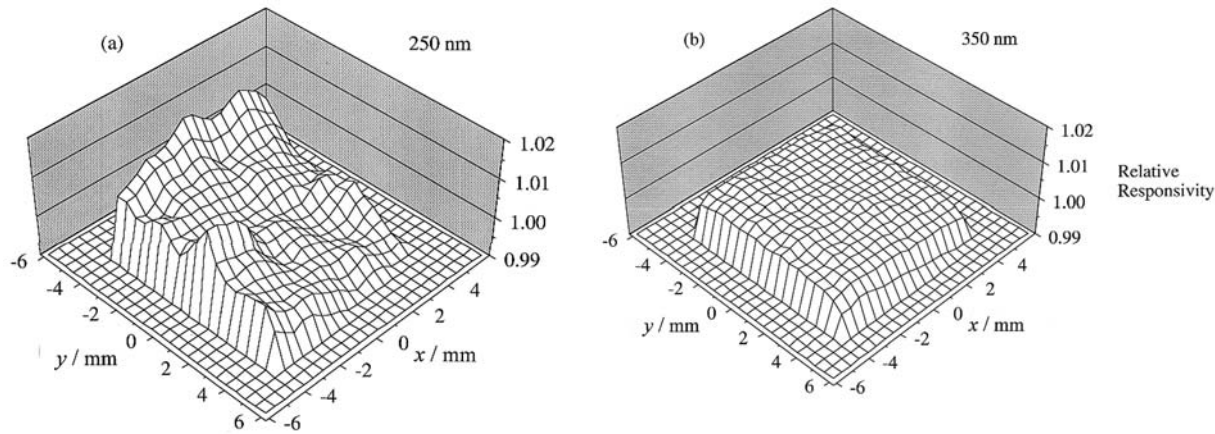


**Figure 9.** Comparison of IRD UVG-100 #1 spatial uniformity at (a) 250 nm and (b) 350 nm.

A long-term study is continuing at the NIST to find new UV detectors with better responsivity uniformity and stability. As part of this study an APA Optics 16 mm<sup>2</sup> GaN photodiode and two IRD UVG-100 1 cm<sup>2</sup> silicon photodiodes have recently been measured for spatial uniformity. Figure 8 shows the GaN photodiode spatial uniformity at (a) 250 nm and (b) 350 nm. The IRD UVG-100 photodiode spatial uniformity is shown at (a) 250 nm and (b) 350 nm in Figure 9.

#### 4. Conclusions

We have shown that photodiode responsivity spatial uniformity can change with wavelength. We have also shown that, although some silicon photodiodes appear uniform over much of their responsivity range, there is a significant change in uniformity as the wavelength approaches the bandgap (1100 nm). The NIST now routinely measures the uniformity at 500 nm and 1000 nm of the silicon photodiodes that are issued to customers for the visible to near-IR spectral region. Photodiodes that show a significant change in uniformity at 1000 nm are not issued. Since non-uniformity can increase the spectral responsivity uncertainties due to changes in alignment and irradiance geometry, the photodiode non-uniformity should be accounted for in the uncertainty budget for spectral responsivity measurements.

**Acknowledgement.** The authors would like to thank George Eppeldauer and Rajeev Gupta for the use of several of the photodiodes included in this paper.

**Note.** Certain commercial equipment, instruments, or materials are identified in this paper to foster understanding. Such identification does not imply recommendation or endorsement by the National Institute of Standards and Technology, nor does it imply that the materials or equipment identified are necessarily the best available for the purpose.

#### References

1. Larason T. C., Bruce S. S., Parr A. C., *Natl. Inst. Stand. Technol. (US), Spec. Publ. 250-41*, 1998.
2. White M. G., Bittar A., *Metrologia*, 1993, **30**, 361-364.
3. Lei F., Fischer J., *Metrologia*, 1993, **30**, 297-303.
4. Köhler R., Goebel R., Pello R., *BIPM Rapport BIPM/94-9*, Sèvres, Bureau International des Poids et Mesures, 1994.
5. Köhler R., Goebel R., Stock M., Pello R., *Proc. SPIE*, 1996, **2815**, 22-30.
6. Fox N. P., Prior T. R., Theocharous E., Mekhontsev S. N., *Metrologia*, 1995/96, **32**, 609-613.
7. Theocharous E., Fox N. P., Prior T. R., *Proc. SPIE*, 1996, **2815**, 56-68.
8. Stock K.D., Heine R., Hofer H., *Metrologia*, 1991, **28**, 207-210.
9. Livigni D., Li X., *Proc. NCSL 1995 Workshop and Symposium*, 1994, 337-352.
10. Gullikson E. M., Korde R., Canfield L. R., Vest R. E., *J. Elect. Spect. Rel. Phenom.*, 1996, **80**, 313-316.
11. Stock K. D., *Appl. Opt.*, 1988, **27**, 12-14.
12. Schaefer A. R., Zalewski E. F., Geist J., *Appl. Opt.*, 1983, **22**, 1232-1236.
13. Personal communication with Richard Austin of Gamma Scientific.
14. Taylor B. N., Kuyatt C. E., *Natl. Inst. Stand. Technol. (US), Tech. Note 1297*, 1994.